Food and Chemical Toxicology 129 (2019) 365–375

Contents lists available at ScienceDirect

Food and Chemical Toxicology

journal homepage: www.elsevier.com/locate/foodchemtox

Ferulic acid altered IL-17A/IL-17RA interaction and protected against imiquimod-induced psoriasis-like skin injury in mice

Hsin-Yi Lo[a], Chia-Cheng Li[a], Hui-Man Cheng[b,c], I-Chen Liu[a], Tin-Yun Ho[a,d,**], Chien-Yun Hsiang[e,*]

[a] Graduate Institute of Chinese Medicine, China Medical University, Taichung, 40402, Taiwan
[b] School of Chinese Medicine, China Medical University, Taichung, 40402, Taiwan
[c] Department of Chinese Medicine, China Medical University Hospital, Taichung, 40447, Taiwan
[d] Department of Health and Nutrition Biotechnology, Asia University, Taichung, 41354, Taiwan
[e] Department of Microbiology and Immunology, China Medical University, Taichung, 40402, Taiwan

ARTICLE INFO

Keywords:
ferulic acid
Psoriasis
Imiquimod
Interleukin-17
Interleukin-17 receptor

ABSTRACT

Ferulic acid (FA), a phenolic phytochemical, is commonly found in grains, vegetables, and fruits. Interleukin-17A (IL-17A) and IL-17 receptor A (IL-17RA) interaction is one of important therapeutic targets for psoriasis. Here we analyzed the FA effects on IL-17A/IL-17RA interaction and psoriasis-like skin injury induced by imiquimod (IMQ). IL-17A-blocking assay and docking analysis showed that FA interacted with Trp-67, Gln-94, and Glu-95 residues of IL-17A via hydrogen bonds and consequently abolished the binding of IL-17RA to IL-17A. Mice were topically given with IMQ and orally given with various amounts of FA for 14 consecutive days. FA attenuated IMQ-induced psoriasis-like skin lesions in a dose-dependent manner, and the epidermal thickness of mice treated with 100 mg/kg FA was reduced by 53.48 ± 4.44% in comparison with sham. Global analysis of differentially expressed genes showed that IMQ and FA significantly affected immune response, metabolism, and mitogen-activated protein kinase signaling pathways. Immunohistochemical staining showed that FA inhibited the infiltration and the cytokine secretion of Th17 cell, dendritic cell, and granulocyte subsets in psoriatic skin tissues. In conclusion, we newly identified that oral administration of FA protected against IMQ-induced psoriatic skin injury in mice. Moreover, its protection was associated with the interference of IL-17A/IL-17RA interaction.

1. Introduction

Ferulic acid (4-hydroxy-3-methoxycinnamic acid) (FA) is an abundant phenolic phytochemical present in plant cell walls. It is most commonly found in grains, vegetables, and fruits, and occurs in particularly high concentrations (approximately 700 mg/kg) in wheat bran and tomatoes (Mattila and Kumpulainen, 2002). It has also been found in Chinese medicine herbs, such as *Angelica sinensis* (Chinese angelica root), and in the tea brewed from the common centaury (Valentão et al., 2001). In addition to being naturally present in foods, FA is also used as a food additive to bask the bitter aftertaste (acesulfame potassium) of the artificial sweetener (Nankar et al., 2017).

FA possesses various pharmacological effects, including anti-oxidative, anti-inflammatory, anti-microbial, and neuroprotective activities (Colombo and Papetti, 2019; Ghosh et al., 2017; Mancuso and Santangelo, 2014; Zhao and Moghadasian, 2008). FA exhibits antioxidant effects and attenuates doxorubicin-induced redox stress and oxidative stress-mediated signal transduction in myocardial cells (Sahu et al., 2019). FA is listed as “antioxidant” in the “food additives” list because it has been reported to maintain color tone of Greenpeace, and prevent the discoloration of green tea and banana (Ou and Kwok, 2004). FA provides protection against hyperglycemia-induced, oxidative stress-mediated splenotoxicity (Ghosh et al., 2018). FA displays neuroprotective activities against oxidative stress-related apoptosis after cerebral ischemia/reperfusion injury in rats (Cheng et al., 2008). FA blocks rotenone-induced dopaminergic neurodegeneration through antioxidant, anti-inflammatory activities, suggesting that FA may be used as potent neuroprotective agent in the prevention of Parkinson's disease (Ojha et al., 2015). FA also plays a vital role as an anti-inflammatory agent in various pathophysiological conditions, such as hepatic inflammation, aortic inflammation, trinitrobenzene sulfonic acid-induced ulcerative colitis, and ultraviolet (UV)–B-induced skin

* Corresponding author. Department of Microbiology and Immunology, China Medical University, No. 91 Hsueh-Shih Road, Taichung, 40402, Taiwan.
** Corresponding author. Graduate Institute of Chinese Medicine, China Medical University, No. 91 Hsueh-Shih Road, Taichung, 40402, Taiwan.
E-mail addresses: tyh@mail.cmu.edu.tw (T.-Y. Ho), cyhsiang@mail.cmu.edu.tw (C.-Y. Hsiang).

https://doi.org/10.1016/j.fct.2019.04.060
Received 5 March 2019; Received in revised form 15 April 2019; Accepted 30 April 2019
Available online 03 May 2019
0278-6915/

Abbreviations

DEGs	differentially expressed genes
DAG	Directed Acyclic Graph
FA	ferulic acid
GO	Gene Ontology
H&E	hematoxylin/eosin
HRP	Horseradish peroxidase
IL-17A	interleukin-17
IL-17RA	interleukin-17 receptor A
IMQ	imiquimod
IHC	immunohistochemical
IL-1β	interleukin-1β
KEGG	Kyoto Encyclopedia of Genes and Genomes
LD50	lethal dosage at 50%
OD	optical density
PBS	phosphate-buffered saline
PCR	polymerase chain reaction
PASI	psoriasis area and severity index
RSEM	RNA-Seq by Expectation Maximization
STAT1	signal transducer and activator of transcription 1
TMB	3,3′,5,5′-tetramethylbenzidine substrate solution
TNF-α	tumor necrosis factor-α
UV	ultraviolet

inflammation (Ambothi et al., 2015; Ghosh et al., 2017).

Psoriasis is a chronic inflammatory skin disease that affects more than 100 million people, approximately 2% of the global population worldwide. Psoriasis is characterized by sharply demarcated, erythematous, scaling plagues that typically affect elbows, knees, scalp, and trunk. Patients with psoriasis have a high risk of developing psoriatic arthritis, metabolic syndrome, and cardiovascular disease (Boehncke and Schon, 2015). The etiology of psoriasis is very complicated; however, current researches indicated that interleukin-17A (IL-17A) plays a crucial role on the pathogenesis of psoriasis (Hawkes et al., 2018a). IL-17A alone or in combination with tumor necrosis factor-α (TNF-α) induces the expression of psoriasis-related genes in keratinocytes. In addition, IL-17A activates the activities of transcription factors, such as nuclear factor-κB (NF-κB) and STAT1 (signal transducer and activator of transcription 1), resulting in the proliferation and the abnormal differentiation of keratinocytes, and the infiltration of immune cells (Hawkes et al., 2018a). Topical therapy (including coal tars, topical corticosteroids, retinoids, and vitamin D analogues), phototherapy, and systemic therapy (including methotrexate, immunosuppressive drug, retinoids, and biologics) have been applied in clinics for the treatment of psoriasis (Conrad and Gilliet, 2018). Although these therapies display beneficial effects on psoriasis, they often cause undesirable adverse effects, such as folliculitis. Moreover, biologics, such as monoclonal antibodies against IL-17A or IL-17 receptor A (IL-17RA), may cause nasopharyngitis, upper respiratory tract infection, transient neutropenia, and gastroenteritis (Armstrong et al., 2013; Cui et al., 2018).

In previous study, we have found that vanillin improves psoriatic inflammation in mice, and the improvement by vanillin is related to the regulation of IL-17 (Cheng et al., 2017). FA is a precursor in the manufacture for the production of aromatic compounds, such as vanillin (Negishi et al., 2009). Recent report indicated that FA inhibits the IL-17A-mediated expression of IL-17RA in fibroblast-like synoviocytes isolated from adjuvant-induced arthritis rats (Ganesan and Rasool, 2019). However, effects of FA on IL-17A/IL-17RA interaction and IL-17A-associated diseases, such as psoriasis, are still unknown. To address this question, we evaluated the effects of FA on the interaction between IL-17A and IL-17RA by IL-17A-blocking assay and docking analysis. The beneficial effect of FA on psoriasiform dermatitis was analyzed in imiquimod (IMQ)-induced mouse model. The improvement of FA on psoriasis-like inflammation was evaluated by macroscopic and microscopic lesions. Anti-psoriatic mechanism of FA was further analyzed by RNA sequencing (RNA-Seq) and immunohistochemical (IHC) staining. Our data showed that FA altered the interaction between IL-17A and IL-17RA, resulting in the amelioration of psoriasiform dermatitis in mice.

2. Materials and methods

2.1. Chemicals

All chemicals, except indicated, were purchased from Sigma-Aldrich (St. Louis, MO). IMQ cream (5%, Aldara®) was purchased from 3M Pharmaceutical (St. Paul, MN). FA was dissolved in water at 10 mg/ml. Petroleum jelly (Vaseline) was purchased from Acros Organics (Pittsburgh, PA). Recombinant IL-17A protein and recombinant IL-17RA protein (Fc chimera active) were purchased from Abcam (Cambridge, MA). Horseradish peroxidase (HRP)-conjugated goat anti-human IgG Fc antibody was purchased from Millipore (Temecula, CA). 3,3′,5,5′-Tetramethylbenzidine substrate solution (TMB) single solution was purchased from Invitrogen (Camarillo, CA). Rabbit polyclonal antibodies against IL-17A and interleukin-1β (IL-1β), and mouse monoclonal antibody against CD11c were purchased from Santa Cruz Biotechnology (Santa Cruz, CA). Rabbit monoclonal antibodies against CD4 and CD11b, rat monoclonal antibody against Gr-1, and rabbit polyclonal antibody against IL-23 were purchased from Abcam (Cambridge, MA).

2.2. IL-17A-blocking assay

Microtiter plates (MaxiSorp Nunc-Immum™ plates, Nunc, Denmark) were coated at 4 °C overnight with 1 ng/well of recombinant IL-17A, which was diluted in phosphate-buffered saline (PBS) (137 mM NaCl, 1.4 mM KH_2PO_4, 4.3 mM Na_2HPO_4, 2.7 mM KCl, pH 7.2). Plates were washed three times with 400 μl/well of PBST (0.5% Tween 20 in PBS), blocked with 100 μl/well of blocking buffer (1% bovine serum albumin in PBST) at room temperature for 1 h, and then incubated with various concentrations of IL-17R (positive control) or FA at room temperature for 1 h. After washing three times with PBST, 50 ng/well of recombinant Fc-tag IL-17RA, which was diluted in blocking buffer, was added and incubated at 37 °C for 2 h. The bound Fc-tag IL-17RA was then detected by adding 100 μl/well of HRP-conjugated goat anti-human IgG Fc antibody (5000 × dilution) at room temperature for 1 h and then 100 μl/well of TMB single solution at room temperature for 30 min. The reaction was stopped by adding 50 μl/well of 2 N H_2SO_4 and the absorbance was read at 405 nm in an ELISA plate reader (Multiskan GO, Thermo Fisher, Waltham, MA). IL-17A-blocking ability was presented by changes in optical density (OD), which was calculated by subtracting absorbance without FA or IL-17RA from absorbance at indicated concentration of FA or IL-17RA.

2.3. Docking analysis

Docking analysis was performed by Swiss-Dock software (http://www.swissdock.ch/). The crystal structure of human IL-17A (PDB ID: 4HR9) was obtained from protein data bank (http://www.rcsb.org/). IL-17A dimer structure was chosen as a target using the target selection tab in SWISS-Dock. The structure of FA was obtained from ZINC (http://zinc.docking.org/, accession number 58258). The binding affinities of binding clusters were evaluated by deltaG (kcal/mol). All docking structure figures were prepared by UCSF Chimera (https://www.cgl.ucsf.edu/chimera/).

2.4. Animal experiment

BALB/cByJ mice (5-6 weeks old, female) were purchased from National Laboratory Animal Center (Taipei, Taiwan). Mouse experiments were conducted under ethics approval from China Medical University Animal Care and Use Committee (Permit number CMUIACUC-2016-034). Mice were maintained under a 12:12 light/dark cycle with free access to water and food.

Mice were randomly divided into five groups of 5–7 mice per group: (1) mock, Vaseline treatment; (2) sham, IMQ induction; (3) FA10, IMQ induction + 10 mg/kg FA treatment; (4) FA50, IMQ induction + 50 mg/kg FA treatment; (5) FA100, IMQ induction + 100 mg/kg FA treatment. Psoriasis-like skin inflammation in mice was induced as described previously (Cheng et al., 2017; van der Fits et al., 2009). Briefly, the hair on the back of mouse was removed by Veet® (Reckitt Benckiser, Massy Cedex, France). Vaseline cream (62.5 mg, mock) or IMQ (62.5 mg, sham) was applied topically on the back skin of mouse with an area of $2 \times 2\,cm^2$ for 14 consecutive days. FA (10, 50, or 100 mg/kg) was ingested daily for two weeks. The severity of inflammation on the dorsal skin was scored according to clinical psoriasis area and severity index (PASI) every two days. Erythema (redness) and desquamation (scaling) were scored blind and independently on a scale from 0 to 4: 0, none; 1, slight; 2, moderate; 3, marked; and 4, very marked. Mice were sacrificed on the 14th day. Skin samples were collected for further experiments.

2.5. Histopathological examination

Skin tissues were fixed in formaldehyde, embedded in parafilm, cut into 4-5 μm-thick sections, and stained with hematoxylin/eosin (H&E). Histopathological changes were assessed by three investigators in a blind fashion. The thickness of epidermis was measured by approximately 40–50 random measurements for each group using ImageScope (Leica Biosystems Imaging, Wetzlar, Germany).

2.6. cDNA library construction and RNA-Seq

Total RNA, extracted from 30 mg of skin tissues by RNeasy Mini Kit (Qiagen, Valencia, CA), was evaluated for RNA concentration and RNA integrity using Agilent 2100 bioanalyzer (Santa Clara, CA). cDNA library was constructed as described previously (Yao et al., 2018). Briefly, total RNA was treated with oligo(dT) magnetic beads to select mRNA. mRNA fragments were reverse-transcribed into double-stranded cDNA using N6 random primers. The synthesized cDNA was subjected to end-repair and 3′ adenylation. Adaptors were ligated to the ends of these 3′ adenylated cDNA fragments, and the ligation products were amplified by polymerase chain reaction (PCR) to enrich the purified cDNA template. The PCR products were then denatured by heat and circularized by the splint oligo sequence. The single-stranded circular DNAs were formatted as the final library. The fragment length distribution in library was validated using Agilent 2100 bioanalyzer and the 150 bp single-end sequencing of qualified library was performed on BGISEQ-500 platform (Shenzhen, China). Raw reads were filtered into clean reads by removing reads with adaptors, reads in which unknown bases were > 10%, or low quality reads (the percentage of low quality bases > 50% in a read) using SOAPnuke software (Chen et al., 2018a). Three biological replicates were used in this study. RNA-Seq data were deposited in NCBI database (BioProject ID: PRJNA523267).

2.7. Reads mapping and functional analysis

Clean reads were aligned and mapped to reference genome using HISAT (Hierarchical Indexing for Spliced Alignment of Transcripts) (Kim et al., 2015; Langmead et al., 2012). Clean reads were further mapped to reference transcripts using Bowtie2 implementation and the gene expression levels were calculated using RSEM (RNA-Seq by Expectation Maximization), a software package for estimating gene and isoform expression levels from RNA-Seq data (Li and Dewey, 2011). Significantly differentially expressed genes (DEGs) were determined using PossionDis, which is based on the Poisson distribution (Audic and Claverie, 1997). The cutoff of DEGs was fold change ≥2 or ≤ −2 and adjusted p value ≤ 0.05. Gene Ontology (GO) functional classification and KEGG (Kyoto Encyclopedia of Genes and Genomes) analysis of DEGs were performed by R program in limma package. GO enrichment result was shown by Directed Acyclic Graph (DAG). Hierarchical clustering analysis of interleukin-related genes was performed and displayed using the WebMeV Multiple Experiment Viewer (http://mev.tm4.org).

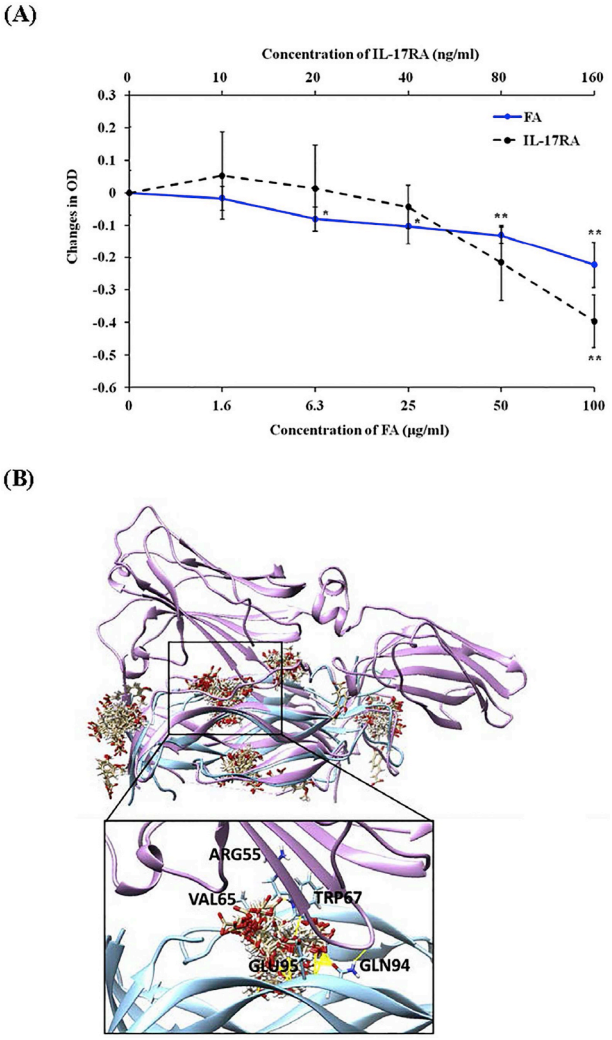

Fig. 1. Potential interaction between FA and IL-17A. (A) IL-17A-blocking assay. Various amounts of IL-17RA and FA were added to IL-17A-coated wells. After incubating for 1 h at room temperature, Fc-tag IL-17RA, HRP-conjugated goat anti-human IgG Fc antibody, and chromatic substrate were sequentially added. The absorbance was read at 405 nm. IL-17A-blocking ability was calculated by subtracting absorbance without IL-17RA or FA from absorbance at indicated concentration of IL-17RA or FA. Values are mean ± standard error of three independent assays. $^{*}p < 0.05$ and $^{**}p < 0.01$, compared to no IL-17RA or FA. (B) Docking of FA with IL-17A using SwissDock. The modeling structure of FA/IL-17A (blue) and the crystal structure of IL-17RA/IL-17A (PDB ID: 4HSA, pink) were superimposed. Enlarged picture shows the FA binding clusters with zoom into the interaction interface of IL-17A with IL-17RA. FA is represented by sticks. Hydrogen bonds between FA and IL-17A are represented by yellow dash lines. (For interpretation of the references to color in this figure legend, the reader is referred to the Web version of this article.)

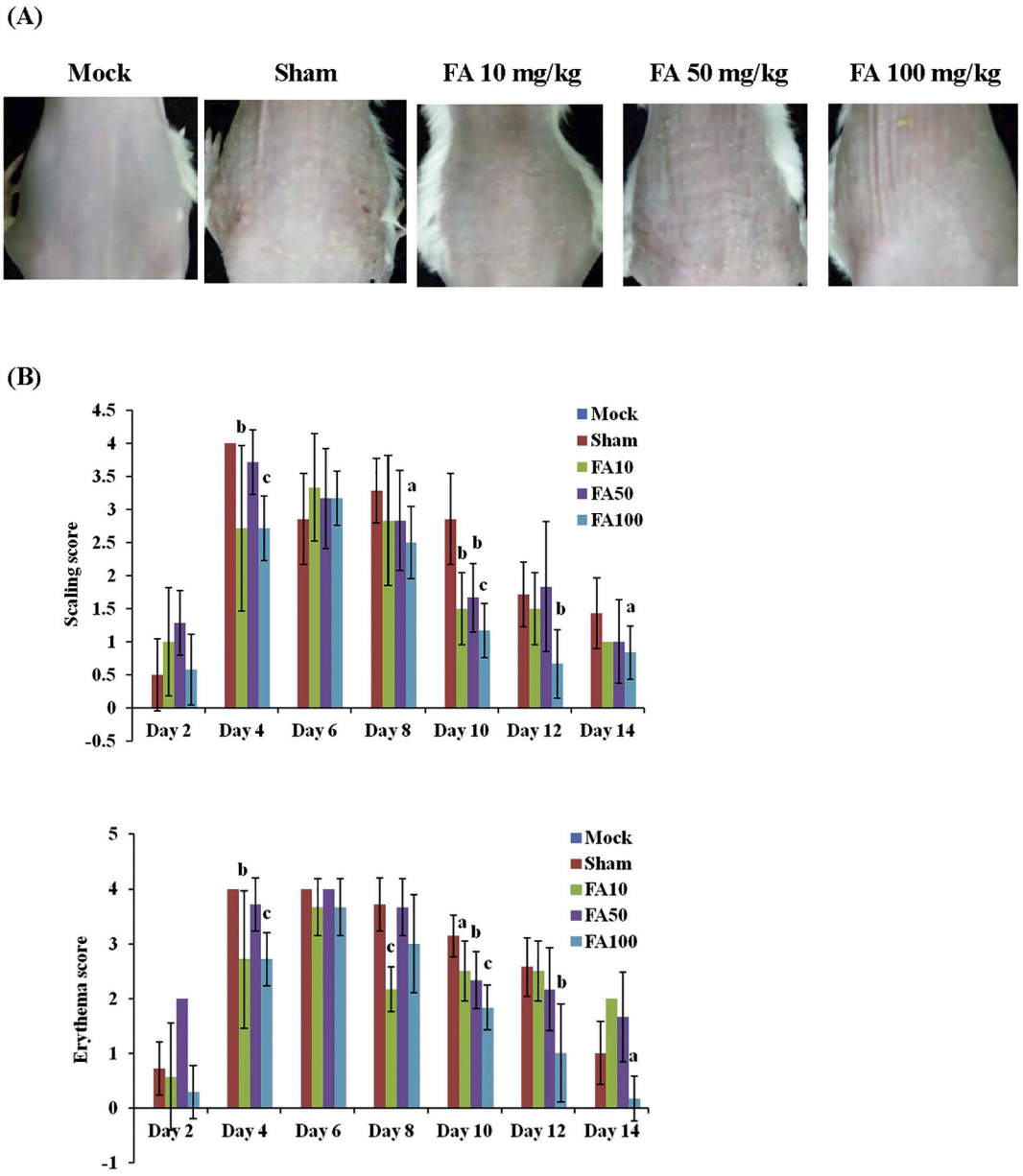

Fig. 2. Effect of FA on IMQ-induced skin lesions in mice. Mice were topically applied with Vaseline (mock) or IMQ (sham) on the dorsal skin and/or given orally with various amounts of FA for 14 consecutive days. (A) Morphological changes of dorsal skin tissues. Photos are representative images (n = 5–7/group). (B) Scaling and erythema scores of dorsal skin lesions. Values are the mean ± standard error. $^{a}p < 0.05$, $^{b}p < 0.01$, and $^{c}p < 0.001$, compared to IMQ group.

2.8. IHC staining

Skin tissue sections (4-5 μm thick) were sequentially incubated with primary antibodies (1:200 dilution) at 4 °C overnight, biotinylated secondary antibody at room temperature for 10 min, and avidin-biotin complex reagent at room temperature for 10 min. The slides were then stained with 3,3′-diaminobenzidine (Histostain-Plus, Invitrogen, Camarillo, CA). IL-17A-, IL-23-, and IL-1β-positive areas were measured using ImageJ (Media Cybernetics, Bethesda, MD) and calculated as (area occupied with brown color/area of whole tissue) × 100. The proportions of CD4-, CD11c-, CD11b-, and Gr-1-positive cells (%) were calculated as (the number of brown cells/the total number of cells) × 100. A total of 100 cells were counted in each view.

2.9. Statistical analysis

Data were presented as mean ± standard error. Data were analyzed by one-way analysis of variance (ANOVA) and post hoc Bonferroni test using SPSS Statistics, version 20 (IBM, Armonk, NY). A p value < 0.05 was considered as statistically significant.

3. Results

3.1. FA altered the interaction between IL-17A and IL-17RA

IL-17A plays a crucial role on the pathogenesis of psoriasis. We wondered whether FA interacted with IL-17A and prevented IL-17A from binding to IL-17RA. IL-17A-blocking assay and docking analysis were therefore performed. IL-17A-blocking assay was a sandwich ELISA that was applied to detect the compound capable of blocking the interaction between IL-17A and IL-17RA. As shown in Fig. 1A, IL-17RA (positive control) bound to IL-17A and consequently abolished the binding of Fc-tag IL-17RA to IL-17A, resulting in the significant decrease of OD values. The presence of FA also significantly decreased the

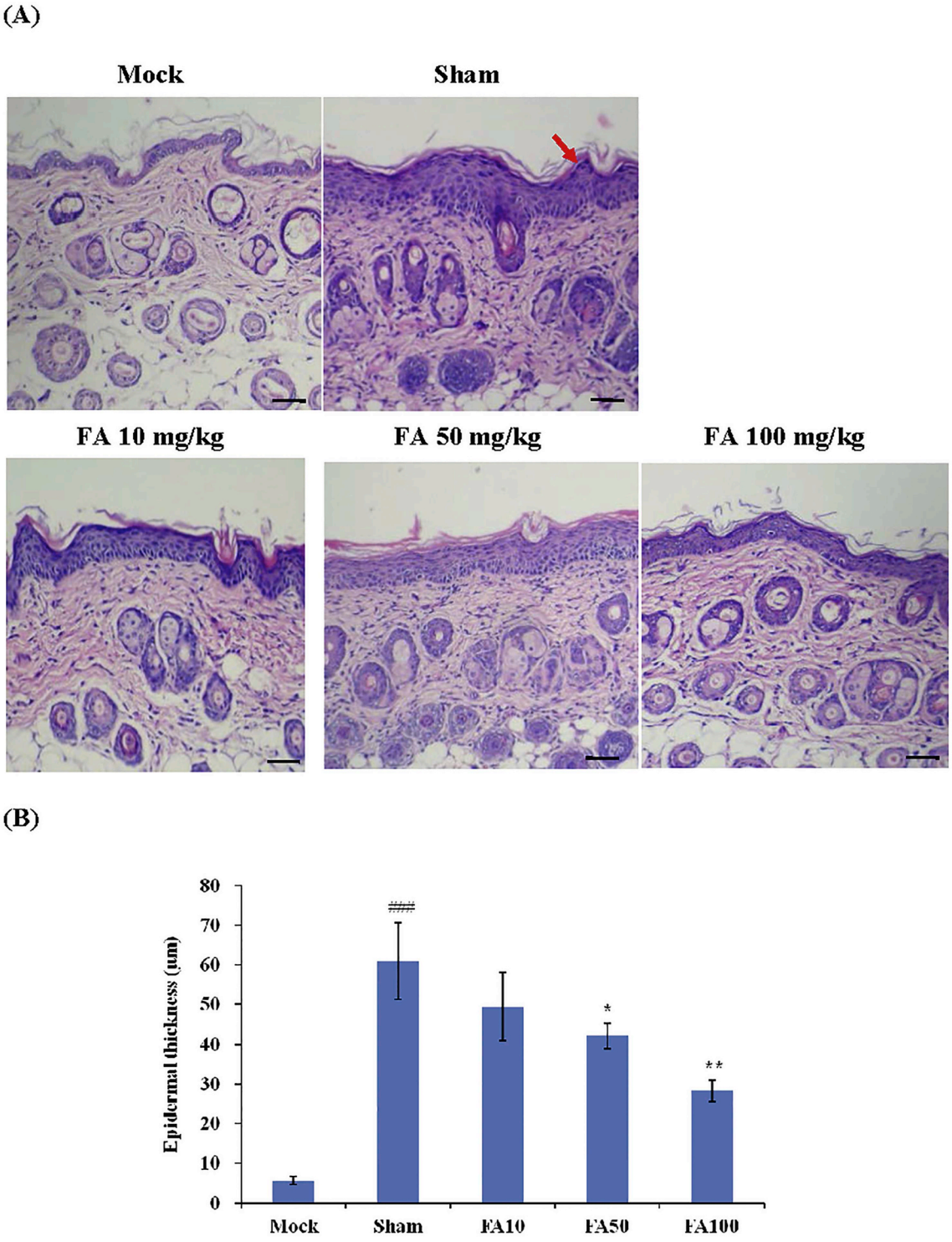

Fig. 3. Effect of FA on IMQ-induced histopathological lesions in mice. Mice were topically applied with Vaseline (mock) or IMQ (sham) on the dorsal skin and/or given orally with various amounts of FA for 14 consecutive days. (A) H&E stain of dorsal skin tissues (original magnification of 200×). Photos are representative histopathological images (n = 5–7 mice/group). Scale bar = 100 μm. The red arrow indicates parakeratosis. (B) Quantification of the thickness of epidermal layer. Data were measured by 40–50 random measurements for each group. Values are mean ± standard error. $^{###}p < 0.001$, compared to mock group. $^{*}p < 0.05$ and $^{**}p < 0.01$, compared to IMQ group. (For interpretation of the references to color in this figure legend, the reader is referred to the Web version of this article.)

OD values and the decrease displayed a dose-dependent manner. These data suggested that FA might interact with IL-17A and altered the IL-17A/IL-17RA interaction. Docking analysis using SwissDock showed that there were 45 probable binding clusters and 256 docking models between FA and IL-17A (Fig. 1B, blue). The average deltaG of 256 docking models was −5.97 ± 0.83 kcal/mol. When the modeling structure of FA/IL-17A was superimposed and compared with the crystal structure of IL-17RA/IL-17A, we found that 11 probable binding clusters and 71 docking models were located on the major binding interface between IL-17RA and IL-17A. The average deltaG was

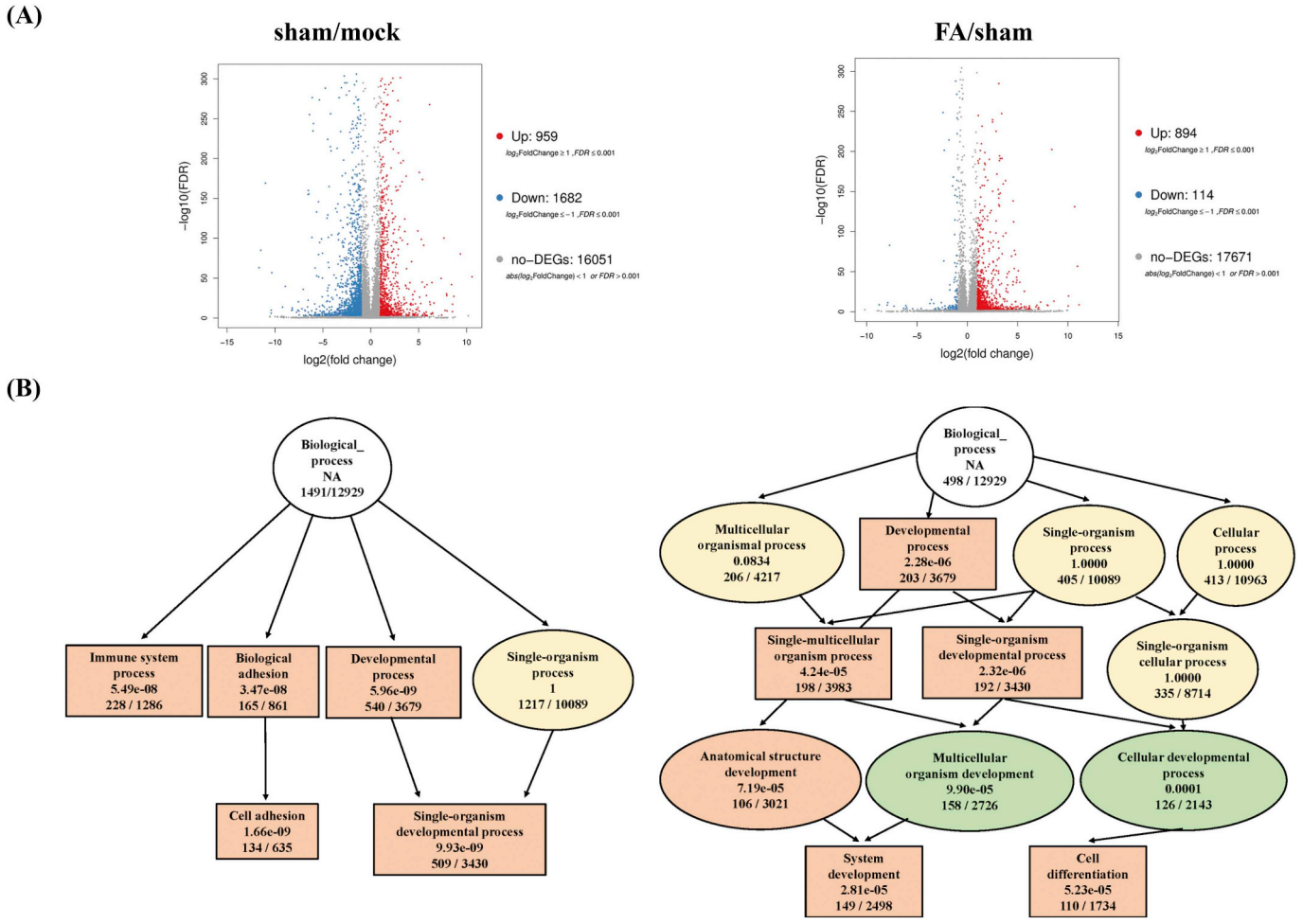

Fig. 4. GO analysis of DEGs affected by IMQ and FA. (A) Volcano plot of DEGs affected by IMQ (left panel) and FA (right panel). X represents $\log_2$ transformed fold change. Y axis represents -$\log_{10}$ transformed significance. Red points represent up-regulated DEGs. Blue points represent down-regulated DEGs. Gray points represent non-DEGs. (B) GO functional enrichment of DEGs affected by IMQ (left panel) and FA (right panel). We used DAG to show the GO enrichment result. Each node shows the name of GO term, *p*-value, and affected gene number/total gene number in the GO term. The darker (red) the color means the lower the *p*-value. (For interpretation of the references to color in this figure legend, the reader is referred to the Web version of this article.)

Table 1
Biological pathways commonly regulated by IMQ and FA.

Pathway	Sham		FA		Classification
	Number of altered genes in the pathway[a]	*p*-value	Number of altered genes in the pathway[a]	*p*-value	
Arachidonic acid metabolism	34 (1.57%)	2.61×10^{-5}	16 (2.01%)	0.0013	Lipid metabolism
Extracellular matrix-receptor interaction	30 (1.39%)	0.0002	12 (1.51%)	0.0242	Signaling molecules and interaction
Glutamatergic synapse	30 (1.39%)	0.0015	13 (1.63%)	0.0106	Nervous system
Mitogen-activated protein kinas signaling pathway	52 (2.4%)	0.0107	24 (3.02%)	0.0069	Signal transduction
Melanogenesis	30 (1.39%)	0.0008	12 (1.51%)	0.0191	Endocrine system
Pantothenate and CoA biosynthesis	6 (0.28%)	0.0279	4 (0.5%)	0.0109	Metabolism of cofactors and vitamins
Platelet activation	39 (1.8%)	0.0007	15 (1.88%)	0.0232	Immune system
Rheumatoid arthritis	29 (1.34%)	1.43×10^{-5}	9 (1.13%)	0.0448	Immune diseases
Tyrosine metabolism	12 (0.55%)	0.0214	7 (0.88%)	0.0084	Amino acid metabolism

[a] The numbers in parentheses represent as (number of altered genes in the pathway/total number of differentially expression genes) × 100.

−6.72 ± 0.71 kcal/mol. In addition, FA interacted with IL-17A residues (Trp-67, Gln-94, and Glu-95) located at the IL-17A/IL-17RA interface via hydrogen bonds. These findings suggested that FA interacted with amino acid residues of IL-17A and affected the interaction between IL-17RA and IL-17A.

3.2. FA attenuated IMQ-induced psoriasis-like skin lesions in mice

Psoriasis is a chronic skin inflammation driven mainly by IL-17A. To analyze the effect of FA on IMQ-induced psoriatic inflammation, we treated topically on the dorsal skin of mice with IMQ and gave mice

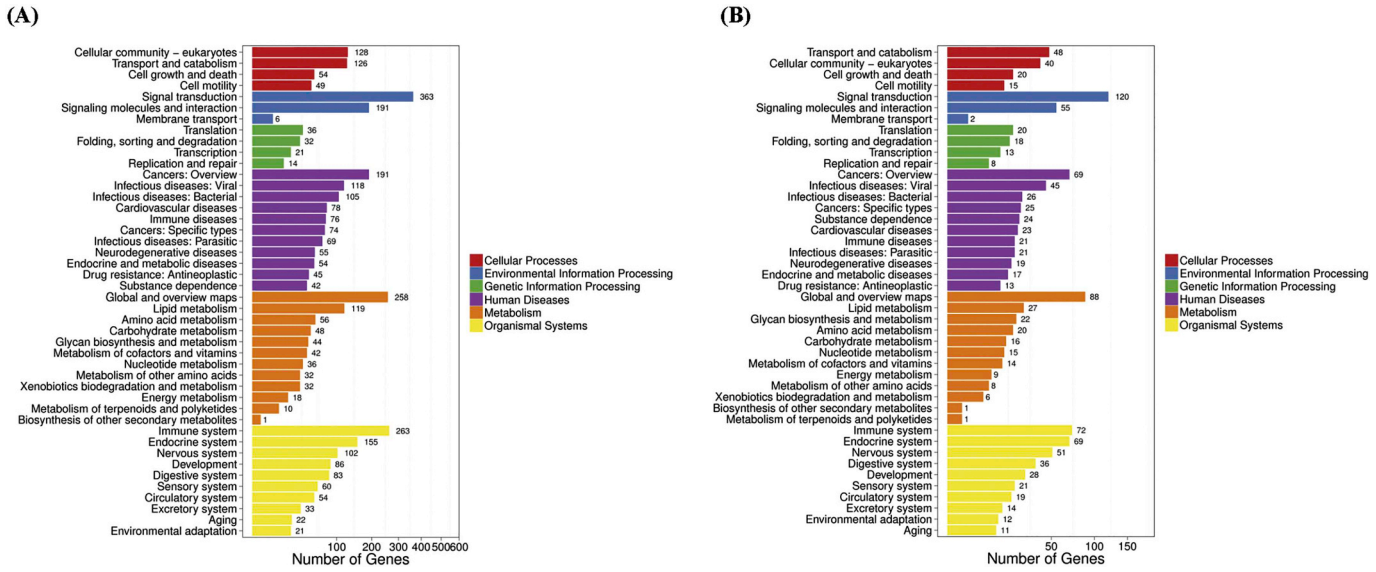

Fig. 5. KEGG classification enrichment analysis of DEGs altered by IMQ and FA. X axis represents number of DEGs. Y axis represents KEGG pathway classification of IMQ (A) and FA (B).

orally with various amounts of FA for 14 consecutive days. The severity of skin inflammation was evaluated according to PASI every two days. As shown in Fig. 2, mice treated with Vaseline alone (mock group) displayed smooth dorsal skin appearances, and no scaling and redness symptoms were observed during the 14-day trial. By contrast, mice treated with IMQ (sham group) displayed rough dorsal skin lesions. The symptoms of scaling and redness were discovered from day 2 onward and the most serious symptoms were appeared on day 4. Administration of FA improved IMQ-induced morphological changes on the dorsal skin of mice from day 4 onward. Fewer symptoms of scaling and redness on the back skin were observed after FA treatment. Moreover, 100 mg/kg FA treatment (FA100 group) significantly ameliorated the skin lesions from day 8 onward.

3.3. FA improved IMQ-induced psoriasis-like histopathological lesions in mice

Histopathological lesions of skin tissues were evaluated by tissue sections stained with H&E. As shown in Fig. 3A, IMQ treatment for 14 days induced psoriasiform lesions, including hyperkeratosis with parakeratosis (red arrow), dilated dermal blood vessels, and inflammatory infiltration. In comparison with mock (5.73 ± 0.97 μm), the thickness of epidermal layer after IMQ treatment was significantly increased (60.92 ± 9.59 μm) (Fig. 3B). In contrast, oral administration of FA improved IMQ-induced histopathological lesions and significantly decreased the thickness of epidermal layer induced by IMQ in a dose-dependent manner. The epidermal thickness of mice treated with 100 mg/kg FA was 28.34 ± 2.71 μm, reduced by 53.48 ± 4.44% in comparison with sham. These data suggested oral administration of FA attenuated IMQ-induced morphological and histopathological changes on the dorsal skin of mice. Moreover, the attenuation of FA displayed a dose-dependent manner.

3.4. Global analysis of DEGs affected by FA in IMQ-treated skin tissues

Sequencing libraries were prepared from skin tissues treated with Vaseline (mock), IMQ (sham), or FA 100 mg/kg (FA). On average, 23.95 Mb total raw sequencing reads were obtained in each group. After filtering out the low quality reads, a total of 23.79 Mb clean reads (1.19 Gb clean bases) were obtained in each group. An average of 93.24% reads (93.08%–93.49%) was mapped to reference genome using HISAT. The uniformity of the mapping result for each sample suggested that the samples were comparable. An average of 81.85% reads was mapped to reference transcripts using Bowtie2 and an average of uniquely mapped reads was 74.84%. A total of 19,143 genes was detected. Using the threshold of fold changes ≥ 2 or ≤ -2 and adjusted p value ≤ 0.05, we identified 2641 DEGs, including 959 up-regulated genes and 1682 down-regulated genes, in IMQ treatment in respect to mock and 1008 DEGs, including 894 up-regulated genes and 114 down-regulated genes, in FA treatment compared to IMQ (Fig. 4A).

3.5. GO annotation and pathway analysis of DEGs altered by FA in IMQ-treated skin tissues

We further analyzed GO classification and functional enrichment of DEGs. Biological processes, including cellular process, single-organism process, metabolic process, biological regulation and response to stimulus, were top five GO classification affected by IMQ and FA (Supporting information Fig. S1). GO functional enrichment analysis showed that IMQ and FA significantly altered 33 and 16 GO terms, respectively (Supporting information Table S1 and Table S2). Development processes, including anatomical structure development, cellular developmental process, multicellular organism development, single-organism developmental process and system development, were significant enriched biological process GO terms commonly affected by IMQ and FA. IMQ significantly altered GO terms belonging to immune responses, such as biological adhesion, cell adhesion, defense response, immune system process, and inflammatory response. DAG of GO enrichment analysis also showed that IMQ affected cell adhesion and single-organism developmental process, while FA altered cell differentiation and system development (Fig. 4B).

Functional enrichment analysis of KEGG pathway showed that 2165 and 796 biological pathways were significantly regulated by IMQ and FA, respectively. Nine pathways were commonly altered by IMQ and FA (Table 1). IMQ and FA significantly affected two immune response-related pathways, including platelet activation and rheumatoid arthritis, and three metabolism-related pathways, including arachidonic acid metabolism, pantothenate and CoA biosynthesis and tyrosine metabolism. Moreover, extracellular matrix-receptor interaction, mitogen-activated protein kinase signaling pathway, and melanogenesis were also altered by both IMQ and FA. Classification enrichment analysis of KEGG pathway further showed that IMQ and FA affected the largest number of genes involved in signal transduction (363 and 120 genes), followed by immune system (263 and 72 genes) and metabolism (258 and 88 genes) (Fig. 5).

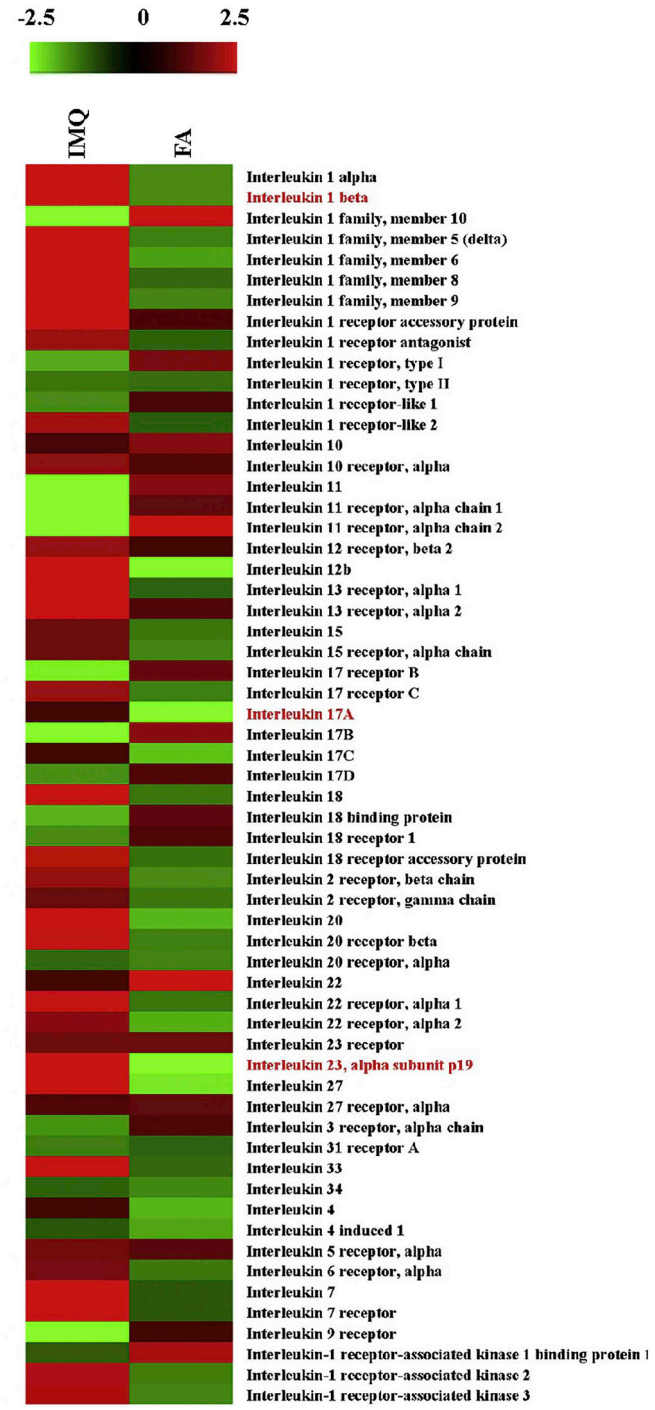

Fig. 6. Hierarchical clustering analysis of interleukin-related gene expression altered by IMQ and FA. The expression of interleukin-related genes affected by IMQ and FA was displayed by hierarchical clustering. Fold changes of genes are color-coded according to the legend on the top. Increased transcript levels are colored red and decreased levels are colored green. (For interpretation of the references to color in this figure legend, the reader is referred to the Web version of this article.)

3.6. FA reduced the expression of interleukin genes and attenuated the infiltration of inflammatory cells in IMQ-induced skin tissues

Because IL-17A/IL-23 axial plays an important role in the pathogenesis of IMQ-induced psoriatic skin inflammation, we analyzed the expression of interleukin-related genes altered by IMQ and FA. Hierarchical clustering analysis showed the opposite images in IMQ and FA treatment (Fig. 6). In a total of 60 interleukin-related genes, the expressions of 38 genes were up-regulated by IMQ, while the majority of IMQ-upregulated gene expressions were down-regulated by FA. By contrast, a total of 22 genes were down-regulated by IMQ, while the majority of IMQ-down-regulated gene expressions were up-regulated by FA. IMQ up-regulated the expression of IL-17A and IL-23 genes by 2.69 and 1.42 folds, while FA down-regulated IMQ-induced IL-17A and IL-23 gene expression with fold changes of −2.35 and −1.60, respectively.

We further applied IHC staining to verify the RNA-Seq results. Antibodies against CD4, CD11c, CD11b, and Gr-1 were used to detect helper T (Th) cells, dendritic cells, leukocytes, and granulocytes, respectively. Th17 cells, IL-23-producing dendritic cells, and granulocytes are considered as key factors for the pathogenesis of psoriasis. The infiltration and cytokine secretion of these cell subsets in psoriasis-like skin was monitored by IHC staining. In comparison to the mock group, IMQ increased the proportions of CD4-and CD11c-positive cells, which were localized in the dermis and the margin between the dermis and epidermis (Fig. 7). IMQ also increased the levels of IL-17A and IL-23, which were localized in both the dermis and epidermis. Additionally, IMQ increased the proportions of CD11b- and Gr-1-positive cells and the levels of proinflammatory cytokine IL-1β, which were mainly localized in the dermis. In contrast to IMQ, FA significantly decreased the proportions of stained cells and the levels of IL-17A, IL-23, and IL-1β in IMQ-induced psoriatic skin tissues. These findings suggested that FA suppressed the infiltration and the cytokine secretion of Th17 cell, dendritic cell, and granulocyte subsets in psoriasis-like skin tissues.

4. Discussion

Psoriasis is an inflammatory skin disorder characterized by multilayered scales with a thickened acanthotic epidermis. Several psoriasis-like murine models, including inducible, transgenic and xenograft types, have been established so far. However, these murine models are associated with significant limitations because of the complex pathogenesis of human psoriasis (Chuang et al., 2018; Hawkes et al., 2018b; Nakajima and Sano, 2018). In this study, we applied IMQ-induced model to analyze the effects of FA on psoriasis-like dermatitis. IMQ-induced model is the most commonly used psoriasis model due to its low cost, convenience, easy to use, and rapid induction of skin inflammation. Nevertheless, this model also has some limitations, such as the relatively nonspecific nature of the induced skin inflammation, unsuitable for chronic use, and non-standardized protocols (Chuang et al., 2018; Hawkes et al., 2018b; Nakajima and Sano, 2018). In addition, psoriasis-like inflammation induced by IMQ would be influenced by genetic background of mice (Bezdek et al., 2017; Flutter and Nestle, 2013; Swindell et al., 2017; van der Fits et al., 2009). BALB/c and C57BL/6 are two common strains used in most studies of IMQ-induced lesions in mouse. Skin inflammation in BALB/c mice develops more rapidly than that in C57BL/6 mice and the systemic side effects, including dehydration and fever, are more severe on C57BL/6 background (van der Fits et al., 2009). However, IMQ-induced gene expression shifts on C57BL/6 background are more consistent with psoriasis than those in BALB/c mice (Swindell et al., 2017). We applied IMQ-induced psoriatic inflammation in BLAB/c mice in this study because it was easier to interpret the skin lesions in light color of skin. Moreover, IMQ induces psoriasis-like lesions with characteristics of scaling and skin thickening via the IL-17 axis, resembling the pathogenesis of human psoriasis.

FA has been applied as a food additive because of its anti-oxidative activity (Nankar et al., 2017). It also plays an important role as an anti-inflammatory agent in various organs by suppressing oxidative stress and regulating cytokine productions. For example, pretreatment of FA protects against acetaminophen-induced acute liver injury by the suppression of Toll-like receptor 4-mediated inflammatory responses in mice (Yuan et al., 2016). FA ameliorates γ-radiation-induced liver inflammation by suppressing the activation of NF-κB, the expressions of

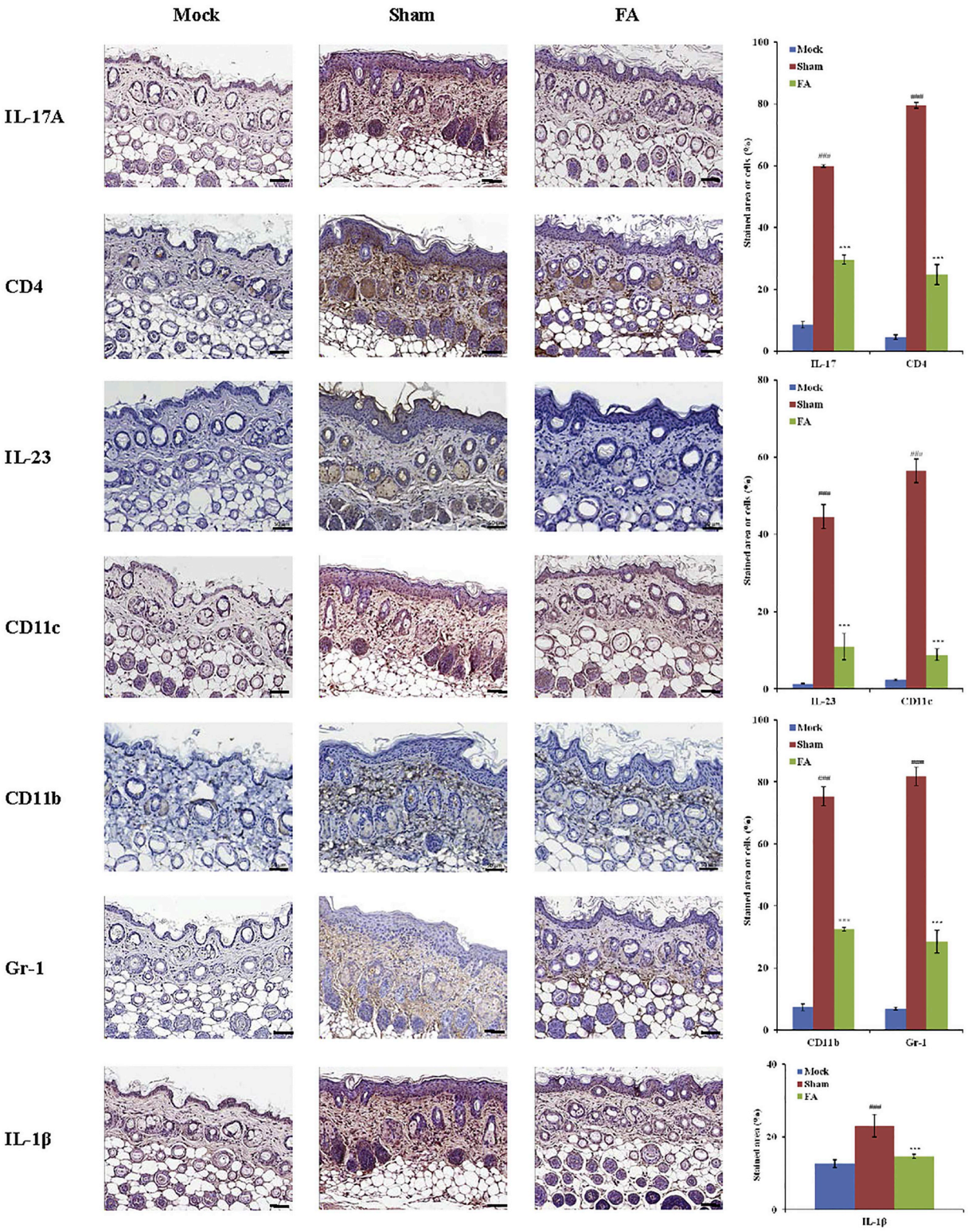

Fig. 7. Effect of FA on the cytokine secretion of specific cell subsets and the infiltration of inflammatory cells in IMQ-induced psoriatic skin tissues. Mice were topically applied with Vaseline (mock) or IMQ (sham) on the dorsal skin and/or given orally with 100 mg/kg FA for 14 consecutive days. Skin sections were stained with antibodies against IL-17A, CD4, IL-23, CD11c, CD11b, Gr-1, and IL-1β. Scale bar = 50 μm. Photos are representative images (n = 5–7/group). Quantification of the stained area or cells (%) is shown on the right panels. Values are mean ± standard error (n = 5–7/group). ###$p < 0.001$, compared to mock group. ***$p < 0.001$, compared to the IMQ group.

TNF-α and IL-6, and the generation of reactive oxygen species in mice (Das et al., 2014). FA also improves ulcerative colitis by decreasing the expression of proinflammatory cytokines (TNF-α, IL-1β, IL-6) and stimulating the expression of anti-inflammatory cytokines (IL-10) in rats (Sadar et al., 2016). Here we newly identified that oral administration of FA suppressed IMQ-induced psoriatic skin inflammation in mice. Moreover, its suppression on skin inflammation was associated with IL-17.

IL-17 is a cytokine whose gene was isolated from a rat-mouse T cell hybridoma in 1993 (Rouvier et al., 1993). So far, six homologous molecules, including IL-17A, IL-17B, IL-17C, IL-17D, IL-17E and IL-17F, have been discovered (Gaffen, 2011). By RNA-Seq analysis, we found that FA decreased the expression of IL-17A gene, the critical cytokine involved in the pathogenesis of psoriasis. By IL-17A-blocking assay, we found that FA interacted with IL-17 and consequently abolished the binding of Fc-tag IL-17RA to IL-17A. By docking analysis, we further found that FA might interact with Trp-67, Gln-94, and Glu-95 residues of IL-17A via hydrogen bonds. The crystal structures of IL-17A and its complex with IL-17RA have been analyzed previously (Liu et al., 2013). Three IL-17RA-binding regions, formed by N-terminal region, central β-strands, and C-domain region of IL-17A, have been designated on the IL-17A homodimer. Trp-67, Gln-94, and Glu-95 residues are located on the central β-strands, the major binding interface between IL-17A and IL-17RA. In addition, mutation at Trp-67 causes a 1.5-fold increase in dissociation constant relative to the recombinant wild-type cytokine, suggesting that Trp-67 of IL-17A is involved in the binding of IL-17RA (Liu et al., 2013). The interaction between FA and Trp-67 of IL-17A might explain why FA decreased the binding of IL-17A to IL-17RA. Moreover, the binding of IL-17A to IL-17RA activates NF-κB and STAT cascades, resulting in the inflammatory gene expression and sequential psoriatic lesion (Hawkes et al., 2018). This phenomenon might explain why FA decreased the expression of cytokine genes, including IL-17 genes, and improved the psoriasis-like skin inflammation in mice.

Previous studies have shown the beneficial effect of FA on skin disorder. For example, FA has been applied as a topical antioxidant to protect skin from UV irritation, such as UV-induced hyperpigmentation and erythema (Saija et al., 2000). It promotes wound healing in diabetic rats via the increase of hydroxyproline and hydroxylysine synthesis, the precursors of collagen (Ghaisas et al., 2014). It inhibits UVB-radiation-induced photocarcinogenesis through modulating inflammatory and apoptotic signaling in Swiss albino mice (Ambothi et al., 2015). It also inhibits tyrosinase activity and melanocytic proliferation, leading to the reduction of melanogenesis (Murray et al., 2008). Interesting, we found that the biological pathways involved in melanogenesis and extracellular matrix-receptor interaction were affected by FA in this study, which was consistent with previous studies. FA is usually applied topically for the management of skin disorder. Our data showed that oral administration of FA ameliorated IMQ-induced psoriatic skin inflammation. However, how did FA affect skin inflammation by oral administration? Recent report studied the pharmacokinetics of herbal extract containing FA in healthy SD rats. Rats were orally given with a single dose of 4.837 g/kg *Hedyotis diffusa Willd* extract (equivalent to 78.58 mg/kg of FA). One and a half hours after oral administration, FA was detected in spleen and liver, with the tissue to plasma concentration ratio of 0.398 ± 0.035 and 0.079 ± 0.003, respectively (Chen et al., 2018b). We proposed that the biodistribution of FA to spleen after ingestion might affect the inflammatory cell population in spleen via disturbing IL-17A/IL-17RA interaction and consequently improve psoriasis-like skin inflammation.

In conclusion, IL-17A and IL-17RA interaction is one of important therapeutic targets for psoriasis. Secukinumab and ixekizumab are IL-17A antagonists that neutralize IL-17A and improve the clinical symptoms of psoriasis, while brodalumab is an IL-17RA antagonist that blocks IL-17RA and displays significant skin clearance (Hawkes et al., 2018). In this study, we newly identified that, in addition to the regulation of cytokine production, FA might interact with IL-17A, prevent IL-17A from binding to IL-17RA, and consequently improve psoriasis-like skin inflammation. FA is a safety food additive, with the oral lethal dosage at 50% (LD50) of approximately 2 g/kg in rats (Ou et al., 2004), equivalent to 4 g/kg in mice. Our data showed that FA ameliorated IMQ-induced psoriasis-like lesions at 100 mg/kg, a dosage below LD50. Therefore, our findings suggested that FA was a bioactive compound against psoriasis-like skin inflammation with low toxicity.

Funding

This work was supported by grants from Ministry of Science and Technology, Taiwan (MOST105-2320-B-039-017-MY3 and MOST107-2320-B-039-029-MY3) and China Medical University, Taiwan (CMU104-H-01 and CMU104-H-02).

Notes

The authors declare no competing financial interest.

Declaration of interests

The authors declare that they have no known competing financial interests or personal relationships that could have appeared to influence the work reported in this paper.

Appendix A. Supplementary data

Supplementary data to this article can be found online at https://doi.org/10.1016/j.fct.2019.04.060.

References

Ambothi, K., Prasad, N.R., Balupillai, A., 2015. Ferulic acid inhibits UVB-radiation induced photocarcinogenesis through modulating inflammatory and apoptotic signaling in Swiss albino mice. Food Chem. Toxicol. 82, 72–78.
Armstrong, A.W., Robertson, A.D., Wu, J., Schupp, C., Lebwohl, M.G., 2013. Undertreatment, treatment trends, and treatment dissatisfaction among patients with psoriasis and psoriatic arthritis in the United States: findings from the National Psoriasis Foundation surveys, 2003-2011. JAMA Dermatol 149, 1180–1185.
Audic, S., Claverie, J.M., 1997. The significance of digital gene expression profiles. Genome Res. 7, 986–995.
Bezdek, S., Hdnah, A., Sezin, T., Mousavi, S., Zillikens, D., Ibrahim, S., Ludwig, R.J., Sadik, C.D., 2017. The genetic difference between C57Bl/6J and C57Bl/6N mice significantly impacts Aldara™-induced psoriasiform dermatitis. Exp. Dermatol. 26, 349–351.
Boehncke, W.H., Schon, M.P., 2015. Psoriasis. Lancet 386, 983–994.
Chen, X., Zhu, P., Liu, B., Wei, L., Xu, Y., 2018b. Simultaneous determination of fourteen compounds of *Hedyotis diffusa Willd* extract in rats by UHPLC-MS/MS method: application to pharmacokinetics and tissue distribution study. J. Pharm. Biomed. Anal. 159, 490–512.
Chen, Y., Chen, Y., Shi, C., Huang, Z., Zhang, Y., Li, S., Li, Y., Ye, J., Yu, C., Li, Z., Zhang, X., Wang, J., Yang, H., Fang, L., Chen, Q., 2018a. SOAPnuke: a MapReduce acceleration-supported software for integrated quality control and preprocessing of high-throughput sequencing data. GigaScience 7, 1–6.
Cheng, C.Y., Su, S.Y., Tang, N.Y., Ho, T.Y., Chiang, S.Y., Hsieh, C.L., 2008. Ferulic acid provides neuroprotection against oxidative stress-related apoptosis after cerebral ischemia/reperfusion injury by inhibiting ICAM-1 mRNA expression in rats. Brain Res. 1209, 136–150.
Cheng, H.M., Chen, F.,Y., Li, C.C., Lo, H.Y., Liao, Y.F., Ho, T.Y., Hsiang, C.Y., 2017. Oral administration of vanillin improves imiquimod-induced psoriatic skin inflammation in mice. J. Agric. Food Chem. 65, 10233–10242.
Chuang, S.Y., Lin, C.H., Sung, C.T., Fang, J.Y., 2018. Murine models of psoriasis and their usefulness for drug discovery. Expert Opin. Drug Discov. 13, 551–562.
Colombo, R., Papetti, A., 2019. An outlook on the role of decaffeinated coffee in neurodegenerative diseases. Crit. Rev. Food Sci. Nutr. 7, 1–20.
Conrad, C., Gilliet, M., 2018. Psoriasis: from pathogenesis to targeted therapies. Clin. Rev. Allergy Immunol. 54, 102–113.
Cui, L., Chen, R., Subedi, S., Yu, Q., Gong, Y., Chen, Z., Shi, Y., 2018. Efficacy and safety of biologics targeting IL-17 and IL-23 in the treatment of moderate-to-severe plaque psoriasis: a systematic review and meta-analysis of randomized controlled trials. Int. Immunopharmacol. 62, 46–58.
Das, U., Manna, K., Sinha, M., Datta, S., Das, D.K., Chakraborty, A., Ghosh, M., Saha, K.D., Dey, S., 2014. Role of ferulic acid in the amelioration of ionizing radiation induced inflammation: a murine model. PLoS One 9, e97599.
Flutter, B., Nestle, F.O., 2013. TLRs to cytokines: mechanistic insights from the imiquimod mouse model of psoriasis. Eur. J. Immunol. 43, 3138–3146.
Gaffen, S.L., 2011. Recent advances in the IL-17 cytokine family. Curr. Opin. Immunol. 23, 613–619.
Ganesan, R., Rasool, M., 2019. Ferulic acid inhibits interleukin 17-dependent expression of nodal pathogenic mediators in fibroblast-like synoviocytes of rheumatoid arthritis. J. Cell. Biochem. 120, 1878–1893.
Ghaisas, M.M., Kshirsagar, S.B., Sahane, R.S., 2014. Evaluation of wound healing activity of ferulic acid in diabetic rats. Int. Wound J. 11 523e532.
Ghosh, S., Basak, P., Dutta, S., Chowdhury, S., Sil, P.C., 2017. New insights into the ameliorative effects of ferulic acid in pathophysiological conditions. Food Chem. Toxicol. 103, 41–55.

Ghosh, S., Chowdhury, S., Sarkar, P., Sil, P.C., 2018. Ameliorative role of ferulic acid against diabetes associated oxidative stress induced spleen damage. Food Chem. Toxicol. 118, 272–286.
Hawkes, J.E., Yan, B.Y., Chan, T.C., Krueger, J.G., 2018a. Discovery of the IL-23/IL-17 signaling pathway and the treatment of psoriasis. J. Immunol. 201, 1605–1613.
Hawkes, J.E., Adalsteinsson, J.A., Gudjonsson, J.E., Ward, N.L., 2018b. Research techniques made simple: murine models of human psoriasis. J. Investig. Dermatol. 138, e1–e8.
Kim, D., Langmead, B., Salzberg, S.L., 2015. HISAT: a fast spliced aligner with low memory requirements. Nat. Methods 12, 357–360.
Langmead, B., Salzber, S.L., 2012. Fast gapped-read alignment with Bowtie 2. Nat. Methods 9, 357–359.
Li, B., Dewey, C.N., 2011. RSEM: accurate transcript quantification from RNA-Seq data with or without a reference genome. BMC Bioinf. 12, 323.
Liu, S., Song, X., Chrunyk, B.A., Shanker, S., Hoth, L.R., Marr, E.S., Griffor, M.C., 2013. Crystal structures of interleukin 17A and its complex with IL-17 receptor A. Nat. Commun. 4, 1888.
Mancuso, C., Santangelo, R., 2014. Ferulic acid: pharmacological and toxicological aspects. Food Chem. Toxicol. 65, 185–195.
Mattila, P., Kumpulainen, J., 2002. Determination of free and total phenolic acids in plant-derived foods by HPLC with diode-array detection. J. Agric. Food Chem. 50, 3660–3667.
Murray, J.C., Burch, J.A., Streilein, R.D., Iannacchione, M.A., Hall, R.P., Pinnell, S.R., 2008. A topical antioxidant solution containing vitamins C and E stabilized by ferulic acid provides protection for human skin against damage caused by ultraviolet irradiation. J. Am. Acad. Dermatol. 59, 418–425.
Nakajima, K., Sano, S., 2018. Mouse models of psoriasis and their relevance. J. Dermatol. 45, 252–263.
Nankar, R., Prabhakar, P.K., Doble, M., 2017. Hybrid drug combination: combination of ferulic acid and metformin as anti-diabetic therapy. Phytomedicine 37, 10–13.
Negishi, O., Sugiura, K., Negishi, Y., 2009. Biosynthesis of vanillin via ferulic acid in *Vanilla planifolia*. J. Agric. Food Chem. 57, 9956–9961.
Ojha, S., Javed, H., Azimullah, S., Abul Khair, S.B., Haque, M.E., 2015. Neuroprotective potential of ferulic acid in the rotenone model of Parkinson's disease. Drug Des. Dev. Ther. 9, 5499–5510.
Ou, S., Kwok, K.C., 2004. Ferulic acid: Pharmaceutical functions, preparation and applications in foods. J. Sci. Food Agric. 84, 1261–1269.
Rouvier, E., Luciani, M.F., Mattei, M.G., Denizot, F., Golstein, P., 1993. CTLA-8, cloned from an activated T cell, bearing AU-rich messenger RNA instability sequences, and homologous to a herpesvirus saimiri gene. J. Immunol. 150, 5445–5556.
Sadar, S.S., Vyawahare, N.S., Bodhankar, S.L., 2016. Ferulic acid ameliorates TNBS-induced ulcerative colitis through modulation of cytokines, oxidative stress, iNOs, COX-2, and apoptosis in laboratory rats. EXCLI J 15, 482–499.
Sahu, R., Dua, T.K., Das, S., De Feo, V., Dewanjee, S., 2019. Wheat phenolics suppress doxorubicin-induced cardiotoxicity via inhibition of oxidative stress, MAP kinase activation, NF-κB pathway, PI3K/Akt/mTOR impairment, and cardiac apoptosis. Food Chem. Toxicol. 125, 503–519.
Saija, A., Tomaino, A., Trombetta, D., De Pasquale, A., Uccella, N., Barbuzzi, T., Paolino, D., Bonina, F., 2000. *In vitro* and *in vivo* evaluation of caffeic and ferulic acids as topical photoprotective agents. Int. J. Pharm. 199 39e47.
Swindell, W.R., Michaels, K.A., Sutter, A.J., Diaconu, D., Fritz, Y., Xing, X., Sarkar, M.K., Liang, Y., Tsoi, A., Gudjonsson, J.E., Ward, N.L., 2017. Imiquimod has strain-dependent effects in mice and does not uniquely model human psoriasis. Genome Med. 9, 24.
Valentão, P., Fernandes, E., Carvalho, F., Andrade, P.B., Seabra, R.M., Bastos, M.L., 2001. Antioxidant activity of *Centaurium erythraea* infusion evidenced by its superoxide radical scavenging and xanthine oxidase inhibitory activity. J. Agric. Food Chem. 49, 3476–3479.
van der Fits, L., Mourits, S., Voerman, J.S., Kant, M., Boon, L., Laman, J.D., Cornelissen, F., Mus, A.M., Florencia, E., Prens, E.P., Lubberts, E., 2009. Imiquimodinduced psoriasis-like skin inflammation in mice is mediated via the IL-23/IL-17 axis. J. Immunol. 182, 5836–5845 2009.
Yao, L., Wang, J., Li, B., Meng, Y., Ma, X., Si, E., Ren, P., Yang, K., Shang, X., Wang, H., 2018. Transcriptome sequencing and comparative analysis of differentially-expressed isoforms in the roots of *Halogeton glomeratus* under salt stress. Gene 646, 159–168.
Yuan, J., Ge, K., Mu, J., Rong, J., Zhang, L., Wang, B., Wan, J., Xia, G., 2016. Ferulic acid attenuated acetaminophen-induced hepatotoxicity though down-regulating the cytochrome P 2E1 and inhibiting toll-like receptor 4 signaling-mediated inflammation in mice. Am. J. Transl. Res. 8, 4205–4214.
Zhao, Z., Moghadasian, M.H., 2008. Chemistry, natural sources, dietary intake and pharmacokinetic properties of ferulic acid: a review. Food Chem. 109, 691–702.